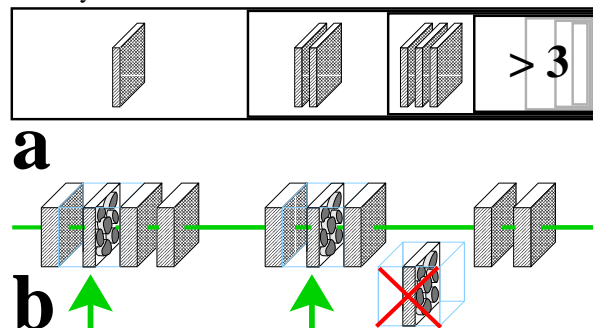


Full Paper: In a series of papers the crystallization of a commercial polyethylene (PE) material is studied by *in situ* ultra small-angle X-ray scattering (USAXS) and it is found that placement of crystallites is predominantly a random car parking process dealt with in the field of random sequential adsorption. Here we investigate the secondary effect, the generation of order from the chaos and characterize how lamellae agglomerate to form clusters. Owing to the chaotic principle, clusters are of different size and thus the nanostructure is, in general, heterogeneous. During isothermal crystallization we only find order inside sparse clusters of lamellae. Globally the nanostructure resembles a random blend of these clusters. A geometric relation couples the number fraction of lamellae to the size of the cluster they belong to. More longitudinal order is achieved, if the material is subsequently quenched. Amorphous gaps of favorable width act as nests in which thin crystals are preferentially generated (harmonic completion). Together with their neighboring parents they imprint excess order. During continuous non-isothermal crystallization we observe that clusters with several members are selectively built from thinner crystals. Order is growing in the late state of crys-

tallization. This violation of the common assumption of homogeneity makes the classic notion of a distorted lattice (convolution polynomial, paracrystal) become restricted to a subset of the global crystallite thickness distribution.



A weak (a) and a strong (b) order generating process found during PE crystallization. The weak process generates a blend of clusters. Within the clusters there is a distorted lattice. The width of the nested boxes show the number fraction of lamellae that belong to clusters of the indicated size. The strong process places new lamellae in the center of a suitable gap.

Oriented quiescent crystallization of polyethylene studied by USAXS.

Part 3: The evolution of crystallite stacking

Norbert Striebeck^{*1}, Armando Almendarez Camarillo¹, Rüdiger K. Bayer²

¹Institute of Technical and Macromolecular Chemistry, University of Hamburg, Bundesstr. 45, 20146 Hamburg, Germany, Fax: +49 40-4123-6008, eMail: Norbert.Striebeck@desy.de

²Institut f. Werkstofftechnik, Universität GH Kassel, 34109 Kassel, Germany

Keywords: crystallization; disorder; lamellar; nanostructure evolution; SAXS

Introduction

The crystallization of polymers, and of polyethylene (PE) in particular, has been studied for almost 50 years. Since that time the nanostructure of alternating crystalline and amorphous layers observed in semicrystalline PE have been associated to a distorted lattice, which is said to cause the long period peak of the small-angle X-ray scattering (SAXS). The probably most well-known descriptions of nanostructure are the stacking model proposed by Hermans^[1] and Hosemann's paracrystalline lattice.^[2,3] Even if both models are able to describe a "destruction of long range order"^[4] with respect to an ideal lattice, the observed distortion is, in general, amazingly strong. As a rule it is impossible to discriminate the two models from each other, and if the size of the layer stacks is studied it is found that only a few lamellae are correlated with each other.^[5-8]

As a result of our time-resolved measurements of oriented quiescent crystallization of polyethylene^[9] we have already demonstrated that the crystallites are predominantly placed at random positions. Thus, in terms of statistical physics, crystallization is dominated by random sequential adsorption (RSA). Not an implied order is distorted, but here and there order grows from the chaos. In this case a general description of real nanostructure with one of the models based on the conception of distorted order does not appear to be appropriate. At best locally, during a certain phase of the process, or on special processing conditions, the classic notions on nanostructure may prevail.

Here, based on the new conception, the complexity of layer arrangement will be analyzed during the course of crystallization as a function of processing conditions. Finally we try to elucidate the conditions that are promoting creation of order.

Theoretical

In part 2^[10] of this series we have discussed the liquid scattering of the ideal random layer system and have shown that its packing correlation is negligible, if the relative width of the crystallite thickness distributions is wide enough. For the commercial material studied here this relation holds fairly well.

A blend of clusters. If crystallization, predominantly, is a random process, but weak correlations are observed beyond the range of packing correlations, then data evaluation tests show that nanostructure is best fitted by a blend of clusters from lamellae, discriminated by different degree of agglomeration (solos, duos, trios, quartets, ...). Each of these clusters is a finite stack described by a classic "distorted lattice". The clusters themselves are, again, randomly distributed on the backbone.

Common features of all clusters. Let r_3 be the direction of the backbone to the crystalline lamellae, and let the isothermal crystallization process be considered. Then we may assume that for all the different degrees of agglomeration the crystal thickness distributions, $h_c(r_3)$, are the same. The same should be valid for the distributions of amorphous gaps, $h_a(r_3)$, which are found in all the clusters made from more than one lamella. Thus the parameter set of the compound model is quite small. For each further component only a weight parameter is added, which is proportional to the number of lamellae that are forming this component. The question of how many degrees of correlation have to be considered can be answered from the range of undulations that are observed in the interface distribution function (IDF)^[9,11] computed from the scattering patterns.

No ambiguity from Babinet's theorem. It is worth to be noted, that in such a model the crystalline domains can uniquely be identified, because the component of the uncorrelated crystallites is subject only to the packing correlation.^[10] This statement is as well valid for the scattering of clusters made from few members only.^[12]

Packing correlations in a blend of clusters. In a blend of clusters we cannot discriminate packing correlation from (poorly) ordered placement, as long as we do not find clusters from at least three lamellae (trios).^[10]

Coupling of cluster fractions. When a cluster fraction model with three or four components is applied to the scattering data from the isothermal crystallization experiment, we find peculiar relations of the weight parameter values. The values appear to be coupled. The coupling observed can be described by a single coupling factor c in a continued fraction model. If n_m is the number fraction of crystallites that are

organized in clusters of m members, then the scattering data indicate the validity of

$$n_m = c(1 - c)^{m-1}, \quad c < 1. \quad (1)$$

Thus clusters with many members are sparse. A sketch demonstrating the relations among the cluster fractions is presented in Figure 1.

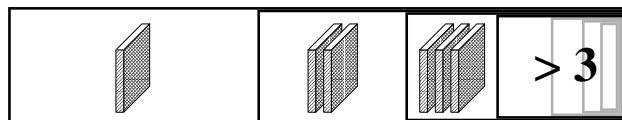


Figure 1: Sketch of the proposed continued-fraction model for the isothermal crystallization and a coupling factor $c = 0.4$. The widths of the nested boxes are proportional to the numbers of crystalline lamellae showing the indicated degree of agglomeration.

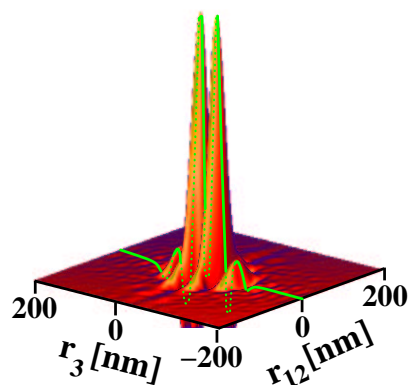


Figure 2: How Ruland's IDF (light line along the meridian) is extracted from multidimensional CDF for analysis of domain arrangement in the direction r_3 , i.e. the fiber axis of semicrystalline PE material. The CDF is the physical space image of inter-domain correlations computed from the USAXS pattern with fiber symmetry (117°C during non-isothermal crystallization (cooling rate: 2°C/min)).

For a value of, e.g., $c = 0.4$ the number fraction of solos is $n_1 = 0.4$. The other 60% of lamellae are agglomerated. From this correlated fraction, again 40% are organized in duos only ($n_2 = 0.24$), the other 60% enjoy a higher degree of agglomeration. Thus for the trios we obtain $n_3 = 0.144$. Continued to infinity, the series of cluster weight parameters is intrinsically computed from a general weight parameter (number of lamellae in the sample) and the coupling parameter c .

Experimental and Data Analysis

Highly oriented polyethylene (PE) rods are prepared from commercial material (Lupolen 6021 D, BASF) by high-pressure injection-molding (HPIM),^[9] melt-annealed in a furnace, and finally crystallized in the synchrotron beam of an

ultra small-angle X-ray scattering (USAXS) beam line (BW4, HASYLAB, Hamburg). In the majority of the experiments the orientation is preserved, although the nanostructure is changing completely. In part 1^[9] of this series both the anisotropic scattering patterns have been interpreted and the multidimensional chord distribution functions (CDFs) have been analyzed.

Starting from the CDFs, $z(r_{12}, r_3)$, discussed in part 1^[9] we now cut out IDFs along the meridian r_3 , as is sketched in Figure 2. In the resulting curves information concerning the arrangement of the crystalline domains and the amorphous gaps along the direction of preferred orientation is stored.

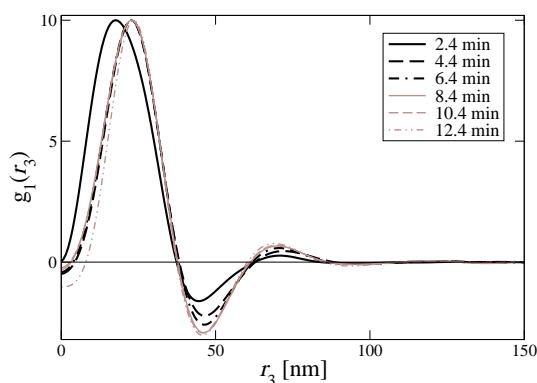


Figure 3: Interface distribution functions (IDFs) during isothermal (127 °C), oriented crystallization after melting at 140 °C.

Results and discussion

Isothermal crystallization

Figure 3 shows the evolution of the IDFs during isothermal crystallization following a temperature jump from 140 °C down to 127 °C. As a function of time, a shift of the peak maximum towards higher layer thicknesses is observed. This finding indicates that during the process the average crystallite thickness at least does not decrease. During the experiment some order is developing among the crystallites which initially are placed at more or less random positions.

Because the IDF computed from the SAXS is closely related to the infinite series of distance distributions between the domains, it is well-suited for the purpose of testing nanostructure models. We have tried to fit the data using the classic models of distorted order, the paracrystalline lattice,^[2] the stacking statistics,^[1] and a model based on the superposition of affinely transformed reference structures combined with a perfect lattice^[13–15] as well as with the aforementioned distorted structures.^[7, 16] None of these models results in a satisfying fit, because the fast decay of the measured functions cannot be described by any of the models discussed in the literature.

Figure 4 demonstrates this behavior. Numbers in parenthesis given in the legend are proportional to the estimated error

of the fit.^[17] A satisfying fit is found, if three kinds of clusters with few members (solos, duos and trios) are superimposed. Even better fits are achieved, if the continued-fraction model from the theoretical section is used (Figure 5). Applied to the data from the isothermal phase of crystallization we find values $0.4 < c < 0.5$ for the coupling constant.

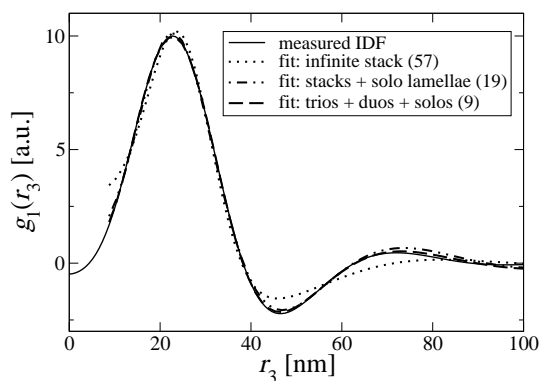


Figure 4: Testing various models for the fit in the case of isothermal crystallization. Interface distribution, $g_1(r_3)$, extracted from the corresponding CDF. The satisfying model is a superposition of clusters with different range of order (single crystalline layers, i.e. “solos”, duos and trios), but all with the same crystalline and amorphous thickness distributions.

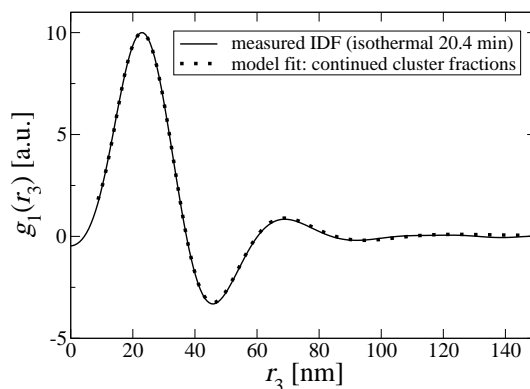


Figure 5: Interface distribution, $g_1(r_3)$, after 20.4 min isothermal crystallization of PE (solid curve), and its fit by the continued cluster fraction model (dotted curve) with $c = 0.4$, i.e. 40% of all lamellae are uncorrelated (cf. Figure 1).

The parameters of the nanostructure extracted from the fits are shown in Figure 6a. During the isothermal phase we observe a constant average crystallite thickness, \bar{t}_c , (filled diamonds) of 28 nm. The fraction n_1 of uncorrelated crystalline lamellae (dotted curve) is close to 50%. In the clusters with several members there are amorphous gaps with almost a constant average thickness (filled circles in Figure 6a). The linear crystallinity, $v_{cl} = \bar{t}_c / (\bar{t}_c + \bar{t}_a)$ in the clusters is 60%. The only significant changes are related to the widths of the layer

thickness distributions (open symbols) that are decreasing during the first 10 min of the isothermal period. The distributions of crystalline thicknesses are not much narrower than the corresponding distributions of the amorphous gaps. Nevertheless, in general the layer thickness distributions found here are the smallest from the series of our experiments. We expect that the trends indicated in Figure 6 could become more clear using an improved data acquisition technique. If we would have had access to a modern CCD detector, we would not have had to sacrifice the possibility to carry out a controlled background subtraction in favor of data with a signal-to-noise ratio that is sufficient for a quantitative analysis.

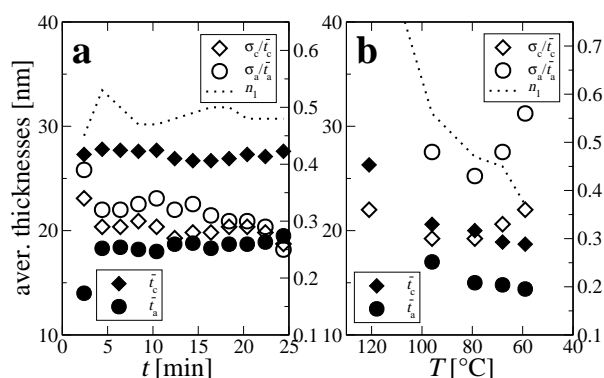


Figure 6: The isothermal crystallization experiment. Nanostructure parameters resulting from the fits on the IDFs. (a) During the isothermal phase. (b) During subsequent rapid cooling (after accidental application of a heating pulse). \bar{t}_c, \bar{t}_a : average thicknesses of crystalline and amorphous layers, respectively. $\sigma_c/\bar{t}_c, \sigma_a/\bar{t}_a$: relative widths of the thickness distributions of the crystalline and amorphous layers, respectively. n_1 : number fraction of uncorrelated crystalline layers.

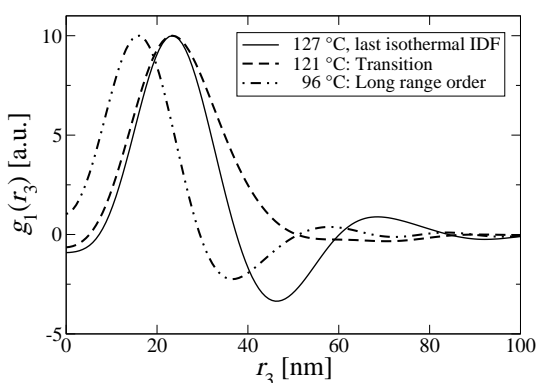


Figure 7: Measured IDFs, $g_1(r_3)$, from the end of the isothermal phase and the beginning of the quenching process. After an intermediate total loss of correlation among the crystallites (121 °C), thinner lamellae are formed that show a rather long ranging correlation, as is recognized from several oscillations in the data taken at 96 °C.

Quenching after isothermal crystallization

When no more change of the scattering pattern has been observed after 30 min in the isothermal phase, the temperature programmer has been switched off in order to use the remaining beam time for the study of structural changes during rapid cooling. Here it must be noted that the following results are affected by an accidental heating pulse of 20 s duration that heated the sample to 135 °C before the quenching process started.

Figure 7 shows IDFs which demonstrate that upon leaving the isothermal phase the nanostructure of the material is changing considerably. After a transition period (dashed curve), during which almost all the correlations among the lamellae appear to be extinguished (heating pulse effect?), long-ranging correlations (dashed-dotted curve) are observed during the whole cooling phase. From now on the continued-fraction model does not fit any more due to its inherent short-range order. During quenching the model made from solo lamellae and an infinite stack fits best, which has already been introduced in Figure 4 (dashed-dotted curve). The structural parameters extracted from the fits are shown in Figure 6b. The number fraction, n_1 , of uncorrelated crystals is considerably decreasing during rapid cooling, and both the average amorphous thickness, \bar{t}_a , and the corresponding crystallite thickness, \bar{t}_c , are decreasing (the latter from 28 nm to 19 nm). The crystallinity v_{cl} is almost constant at 55% throughout the cooling phase. As well interesting is the evolution of the thickness distribution parameters (open symbols). As compared to the isothermal phase, the variations of amorphous and crystalline thicknesses are considerably higher during quenching. Moreover, minima are found at 80 °C, 8 min after the end of the isothermal phase.

Discussing the crystallization process. What conclusions can be drawn from these results concerning the process of crystallization? During the isothermal phase half of the crystals remain uncorrelated. The formation of clusters with some order is weak and sufficiently characterized by the coupling constant c . In this blend of individuals and clusters each domain is given the opportunity to mature best. The average crystallite thickness is slightly increasing, while the crystallite thickness distribution is narrowing. Few clusters from two and more lamellae generate the predominant signal in the discrete small-angle scattering. After this blend is subjected to a short heating pulse followed by rapid quenching, both the fraction of agglomerated domains and the range of correlation is strongly increasing. Moreover, the average crystallite thickness is decreasing considerably. In order to explain the observed homogeneous increase of order, the old crystals must be incorporated into the new longer ranging order. The most simple way to explain this observation is to assume that during quenching the newly generated lamellae are preferentially placed at positions where they complete the existing layers to locally form

some distorted lattice (“harmonic completion”, cf. Figure 8).

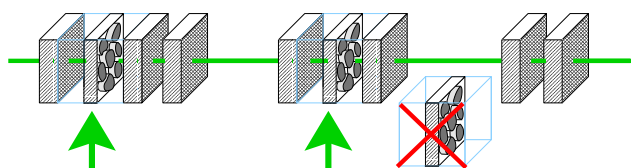


Figure 8: Sketch of a correlation generating insertion process during non-isothermal crystallization. There is a slight preference to insert new (thinner) layers (i.e. block clusters) into the statistical ensemble of the old ones where they fit, i.e. where they generate a local lattice (“harmonic completion”).

In part 1^[9] we have found that these crystallites added during quenching are not yet perfect lamellae, but agglomerates of several blocks. As compared to the isothermal phase these observations may be explained by a process induced by the temperature gradient that causes the crystallites to be frozen-in in a premature state. They thus have neither time to become individually perfect nor to de-correlate from their parents on both sides.

Such a process explains as well, why in the SAXS pattern the long period of the thin lamellae is capable to eclipse the effect of the primary, thick lamellae to such a dominant extent. Not only are *thin* crystals inserted on the backbone. The insertion additionally is carried out in a way that increases the *correlations* among the lamellae and thus increases the corresponding contribution to the discrete scattering considerably.

This finding is in contrast to the results of earlier nanostructure investigations of the processes that form nanostructure during HPIM of the same material.^[18] In the crystallization process under high pressure and an extreme temperature gradient the formation of thin crystallites appears too fast to be supported by suitable nests in an existing layer structure. In this case the placement of the thin lamellae was found to be random, and the only discrete scattering was generated from an initial row structure with a very long spacing.

Finally, it appears worth to be noted that, although during quenching the crystallite thickness distribution is rapidly changing, no decoupling of cluster size and long period is observed. We are going to find such a decoupling effect in the next experiment only.

Nanostructure during non-isothermal crystallization

Figure 9 shows the variation of the IDF during the non-isothermal crystallization experiment with a constant cooling rate of 2°C/min. The first IDF available after crystallization has started shows the particle scattering of crystallites placed at random positions. As a function of decreasing temperature the peaks become narrower and more pronounced. The correlation among crystallites is increasing. For temperatures below 105°C there is little change of the IDF.

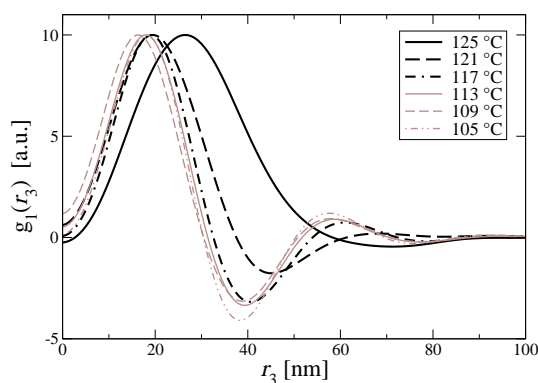


Figure 9: Non-isothermal crystallization with constant slow cooling rate after melting at 140°C. Interface distribution functions (IDFs), $g_1(r_3)$, extracted from the CDFs as indicated in Figure 2 as a function of decreasing temperature.

Analysis of the IDFs. An optimal model is first searched for the data of this experiment, too. Figure 10 shows a typical IDF and three of the models tested.

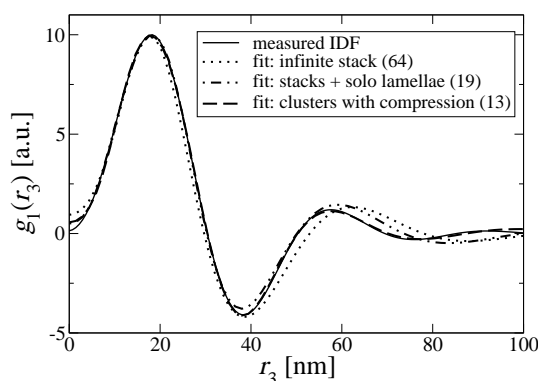


Figure 10: Testing various models for the fit in the case of non-isothermal crystallization with constant low cooling rate. Interface distribution, $g_1(r_3)$, extracted from the corresponding CDF. The best fitting model is, again, a cluster superposition from single crystalline layers, duos and trios). Now correlation between cluster size and lamellar thicknesses is essential for a good fit. Relative change of the fit quality is indicated in parentheses.

Typical for these IDFs is the observation that for $r_3 > 50$ nm the undulations of the classic models are found at r_3 values considerably higher than that of the measured data. There is, again, no classic model that is able to describe such behavior. Applying the novel concept of statistical crystallization with spread clusters, the discrepancy between the established models and the measured data indicates that in the clusters of several members the layers are, in general, thinner than the average solo lamella. We do not know how in a simple and meaningful way to implement this observation in the computer

model. Thus we simply have added an additional compression parameter to the clusters (duos and trios - beyond trios there is no correlation visible). By doing so we assume that the correlated clusters are made from a fractional crystallite thickness distribution which is an affinely compressed image of the total distribution. This model gives reasonable fits, but is physically not as meaningful as the models previously generated (Figure 11).

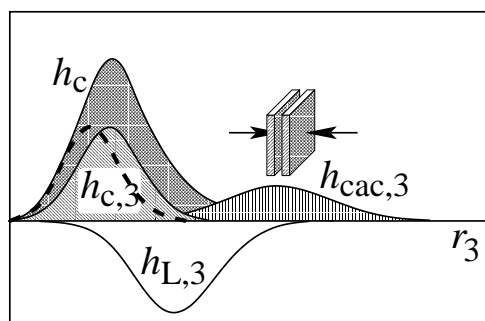


Figure 11: Layer thickness distributions with respect to $g_1(r_3)$, and how we introduced coupling between layer thickness and correlation in the nanostructure model. h_c : Thickness distribution of all crystalline layers. $h_{c,3}$: Thickness distribution of crystalline layers that are members of trios (i.e. clusters of 3 correlated lamellae). The dashed curve indicates what we would suppose to be a better separation between correlated and uncorrelated layers. $h_{L,3}$: The long period distribution of the trios. $h_{cac,3}$: The compressed thickness distribution of the *cac*-sandwiches from inside the trios.

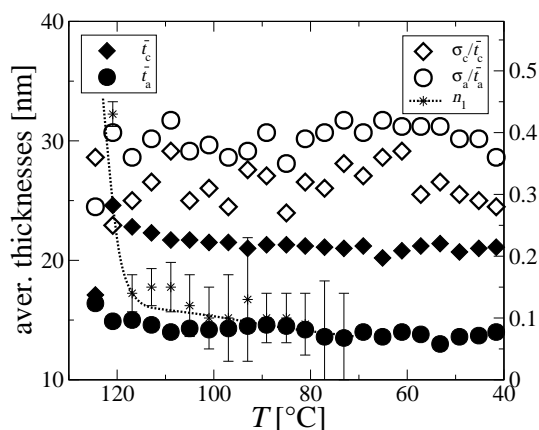


Figure 12: The non-isothermal crystallization experiment. Nanostructure parameters resulting from the fits on the IDFs. \bar{t}_c, \bar{t}_a : average thicknesses of crystalline and amorphous layers from trios, respectively. $\sigma_c/\bar{t}_c, \sigma_a/\bar{t}_a$: relative widths of the thickness distributions of crystalline and amorphous layers, respectively. n_1 : number fraction of uncorrelated crystalline layers (solos).

As is required by the measured data, the distance distribution $h_{cac,3}$ of the trios now has become left-shifted, because no

longer all the crystal lamellae (h_c), but only the thinner lamellae of the trios ($h_{c,3}$) contribute to its formation.

The nanostructure parameters extracted after application of this model are shown in Figure 12. The widths of the layer thickness distributions (open symbols) show that the amorphous gap distributions are somewhat wider than the crystalline thickness distributions. Nevertheless, both distributions are narrower than the ones found in the material during quenching from the isothermal state. During the crystallization experiment the fraction of uncorrelated crystalline lamellae is decreasing from 94% in the beginning to 5% at room temperature. Thus the temperature ramp is, ultimately, enforcing correlations for almost all lamellae. During the process the system is continuously transformed from a random particle system into a cluster system that, predominantly, is made from duos and trios with the trios showing smaller long periods than the duos. Initially the long period of the trios is smaller by 20% than that of the duos. During crystallization the compression of the trio long periods is continuously decreasing to 12%. The decrease of the average crystallite thickness \bar{t}_c (filled diamonds) is continuous, the average amorphous thickness (filled circles) cannot be determined with high accuracy as long as the solo component is still significant for the fit.

Conclusions

In our study we have been led to a novel description of crystallization in a polymer, according to which nanostructure is, primarily, the evolution of some limited order from chaotic crowding. Under this premise heterogeneity of nanostructure can be expected, and the classic models of distorted order take a seat in the second row, where they describe clusters from crystals with different degree of agglomeration. The properties of these local nanostructures themselves may depend both on the number of agglomerated crystallites contained, and on their time of creation in the course of the process controlled by temperature and pressure.

Weak order may obviously emerge during the isothermal crystallization even from a weak and unspecified interaction principle, nevertheless its result are only very few clusters containing several members. A basic principle for the generation of stronger order under a temperature gradient appears to be a harmonic completion. If a narrow crystallite thickness distribution is prepared and the crystallites are randomly distributed (isothermal phase), then in a subsequent quenching process first the wide, and later continuously narrower amorphous gaps become preferred nests for thin crystals. After their generation they form a distorted lattice in which their parents are included. If, on the other hand, the material is continuously cooled from the melt, suitable nests have to be formed during the cooling period itself and begin to be effective only after a certain population density of crystals is reached. In this case there is a high probability that at least one of the parents is a thin crystal as

well, and the completed structure (trio) has a lower long period and outer size than the one expected from the classic convolution polynomial construction based on the total distributions of crystal thicknesses and amorphous gaps.

The quality of scattering data could considerably be improved, if advanced X-ray detectors would become available. In particular close to the melt-annealing temperature, in the beginning of crystallization, and during quenching more in-depth information on the nanostructure evolution process could be retrieved.

Acknowledgments. We gratefully acknowledge the Deutsche Elektronen Synchrotron (DESY) for provision of synchrotron radiation facilities at HASYLAB and we would like to thank Sabine Cunis for assistance in using beamline BW4 within the frame of the project II-01-041. One of us (A.A.C.) expresses his gratitude to the Deutscher Akademischer Austauschdienst (DAAD) for an awarded grant, which enables his stay at the University of Hamburg, Germany.

References

- [1] Hermans, J. J.; *Rec. Trav. Chim. Pays-Bas* **1944**; 63, 211.
- [2] Hosemann, R. Bagchi, S. N.; *Direct Analysis of Diffraction by Matter*; Amsterdam: North-Holland; **1962**.
- [3] Hosemann, R.; *Polymer* **1962**; 3, 349.
- [4] Crist, B.; *J. Polym. Sci., Part B: Polym. Phys.* **1973**; 11, 635.
- [5] Kilian, H. G. Wenig, W.; *J. Macromol. Sci. - Phys.* **1974**; B9, 463.
- [6] Santa Cruz, C. Stribeck, N. Zachmann, H. G. Baltá Calleja, F. J.; *Macromolecules* **1991**; 24, 5980.
- [7] Stribeck, N.; *Colloid Polym. Sci.* **1993**; 271, 1007.
- [8] Murthy, N. S. Bednarczyk, C. Moore, R. A. F. Grubb, D. T.; *J. Polym. Sci., Part B: Polym. Phys.* **1996**; 34, 821.
- [9] Stribeck, N. Almendarez Camarillo, A. Cunis, S. Bayer, R. K. Gehrke, R.; *Macromol. Chem. Phys.* **2004**; submitted.
- [10] Stribeck, N.; *Macromol. Chem. Phys.* **2004**; submitted.
- [11] Ruland, W.; *Colloid Polym. Sci.* **1977**; 255, 417.
- [12] Brämer, R. Kilian, H. G.; *Kolloid-Z. u. Z. Polymere* **1972**; 250, 410.
- [13] Porod, G.; *Kolloid-Z.* **1951**; 124, 83.
- [14] Strobl, G. R. Müller, N.; *J. Polym. Sci., Part B: Polym. Phys.* **1973**; 11, 1219.
- [15] Stribeck, N. Ruland, W.; *J. Appl. Cryst.* **1978**; 11, 535.
- [16] Stribeck, N.; *J. Phys. IV* **1993**; 3, 507.
- [17] Draper, N. R. Smith, H.; *Applied Regression Analysis, Second Edition*; New York: John Wiley & Sons; **1980**.
- [18] Stribeck, N. Bayer, R. von Krosigk, G. Gehrke, R.; *Polymer* **2002**; 43, 3779.

Synopsis. Crystallization of PE along a shish is found to be more or less a “car parking problem”. Deviations from this random process are related to order generating processes. Two of these processes are identified: A weak process just generates a blend of clusters, a stronger one is only active during non-isothermal crystallization and makes use of “nests” in which crystals of suitable thickness like to grow and generate order.